UNCONVENTIONAL RESOURCES TECHNOLOGY CONFERENCE
FUELED BY SPE • AAPG • SEG

URTeC: 3848106

A New Approach to Apply Decline-Curve Analysis for Tight-Oil Reservoirs Producing Under Variable Pressure Conditions

Leopoldo M. Ruiz Maraggi*[1], Mark P. Walsh[2], and Larry W. Lake[2].
1. Bureau of Economic Geology, The University of Texas at Austin.
2. Hildebrand Department of Petroleum and Geosystems Engineering, The University of Texas at Austin.

This paper was prepared for presentation at the Unconventional Resources Technology Conference held in Denver, Colorado, USA, 13-15 June 2023.

Abstract

Decline-curve models inherently assume that the bottomhole flowing pressure (BHP) is constant. This is a poor assumption for many unconventional wells. For this reason, the application of decline-curve models might lead to incorrect: (a) flow regime identification and (b) estimated ultimate recovery (EUR). This work presents a novel technique that combines variable BHP conditions with decline-curve models and compares its results with traditional decline-curve analysis (DCA) for both synthetic and tight-oil wells.

Using superposition, we generate a synthetic rate example using the constant-pressure solution of the diffusivity equation for a slightly compressible fluid (decline-curve model) along with a BHP history. However, we validate the technique using incorrect bottomhole and initial reservoir pressures. In each iteration, the algorithm sequentially estimates: (1) the decline-curve model parameters, (2) the BHP, and (3) the initial reservoir pressure. The result of the synthetic example leads to an accurate production history-match and corrected estimates of the initial reservoir pressure and the BHP. Finally, this work compares the results of the technique with traditional DCA in terms of: (a) the model parameters, (b) flow regime identification, (c) production history-matches, and (d) estimated ultimate recovery (EUR) for tight-oil wells using three decline-curve models: 1-D single-phase constant-pressure solution of the diffusivity equation for a slightly compressible fluid, logistic growth model, and Arps hyperbolic relation.

For the synthetic case, the algorithm can estimate the model parameters and the true initial reservoir pressure within 2% error. In addition, the method regenerates the true BHP history and provides an excellent production history-match. The analysis of the tight-oil wells shows that the new approach clearly identifies the flow regimes present in the well, which can be difficult to detect using traditional DCA when the BHP varies. In contrast, the application of traditional DCA shows considerable errors in the estimation of the model's parameters and a poor history-match of the production data. Finally, this work shows that incorporating variable BHP into the decline-curve models leads to more accurate production history-matches and EUR values compared to using only rate-time data.

This paper illustrates a workflow to incorporate variable BHP conditions for any decline-curve model. Moreover, the approach provides improved estimates of the BHP and initial reservoir pressures. The technique is computationally fast and history-matches and forecasts production of unconventional wells more accurately than traditional DCA. The major contribution of this work is the remarkable simplicity yet robustness of our solution to variable pressure decline-curve analysis.

Introduction

Decline-curve analysis is one of the most widely used methods in the oil and gas industry to forecast production from wells. The basic procedure is to establish a trend in the production rate decline, based on the available history, and then extrapolate the decline into the future.

Decline-curve models include the popular Arps hyperbolic model (Arps 1945) as well as the more recent proliferation of decline-curve models developed specifically for unconventional wells, such as the power-law exponential (Ilk et al. 2008), stretched exponential (Valko 2009), and the logistic growth (Clark et al. 2011) models. The recent models include physics-based decline-curve models (Wattenbarger et al. 1998; Patzek et al. 2013; Male et al. 2016).

All these models have one thing in common; namely, they inherently assume a constant BHP. While this assumption is often satisfactory for many conventional-recovery applications, it is often poor for unconventional-recovery applications. If applied to unconventional wells without properly correcting for a variable BHP, rate-time models might—and we show that they will—lead to several inaccuracies, including but not limited to grossly erroneous EURs and improper flow regime identification.

One way to account for variable BHP conditions is to use rate-pressure deconvolution (Kuchuk et al. 2010). This mathematical operation transforms a variable-pressure rate into a constant-pressure rate response. Once we have the constant-pressure response, we fit the rate-time model to it, and then apply convolution to include back pressure variations to history-match and forecast production in the variable-pressure domain. Kuchuk et al. (2005) present an inverse scheme that uses an explicit positivity constrain transforming the linear inversion into non-linear problem. Ilk et al. (2007) introduce a rate-pressure deconvolution approach based on the cumulative production. They propose an inversion scheme using b-spline basis functions with regularization (smoothing) to obtain the constant unit rate solution. The problem with deconvolution approaches is that errors in the data (rate, initial reservoir pressure, and BHP) lead to a convolution matrix which is usually rank deficient and ill-conditioned, making the constant-pressure rate response highly oscillatory and unstable (Aster et al. 2019; Hansen 2010).

A simpler way to account for variable pressure conditions is to use a decline-curve model along with the time-superposition principle. Ilk and Blasingame (2013) and later Collins et al. (2014) propose applying time superposition along with decline-curve models to history-match and forecast production of unconventional wells subject to variable BHPs. The authors note the limitations of the method by pointing out that the superposition principle is only applicable under correct and consistent rate and pressure data. Errors in rate and pressure data lead to poor production history-matches and forecasts.

The goal of this work is to incorporate variable BHP conditions into decline curve models in a fast and simple way while accounting for possible errors in the initial reservoir pressure and BHP history. The technique sequentially estimates: (1) the decline-curve model parameters, (2) the BHP, and (3) the initial reservoir pressure. These parameters are selected so as to accurately history-match the production of tight-oil wells subject to variable pressure conditions.

This paper is organized as follows. First, we detail the steps of the proposed approach. Second, we validate the technique with a synthetic case that has errors in the initial reservoir pressure and BHP history. Finally, this work compares the results of the application of the variable pressure drop DCA and the traditional DCA for tight-oil wells using three decline-curve models: 1-D single-phase constant-pressure solution of the diffusivity equation for a slightly compressible fluid, logistic growth model, and Arps hyperbolic relation.

Methods

Figure 1 is a schematic illustrating the main idea of the variable pressure DCA method and it depicts two pressure domains: constant and variable pressure. Figure 1a depicts the constant-pressure domain, where the decline-curve model's rate history is customarily displayed in terms of the unit-pressure rate, $q_{up}(t;x)$, which is a function of time t and parameters x. Figure 1b shows the variable-pressure domain where the actual rate history displayed. The goal of this step is to map a decline-curve model from a constant pressure drop domain (Fig. 1a) to variable pressure drop domain (Fig 1b) while yielding a good match of the actual rate history.

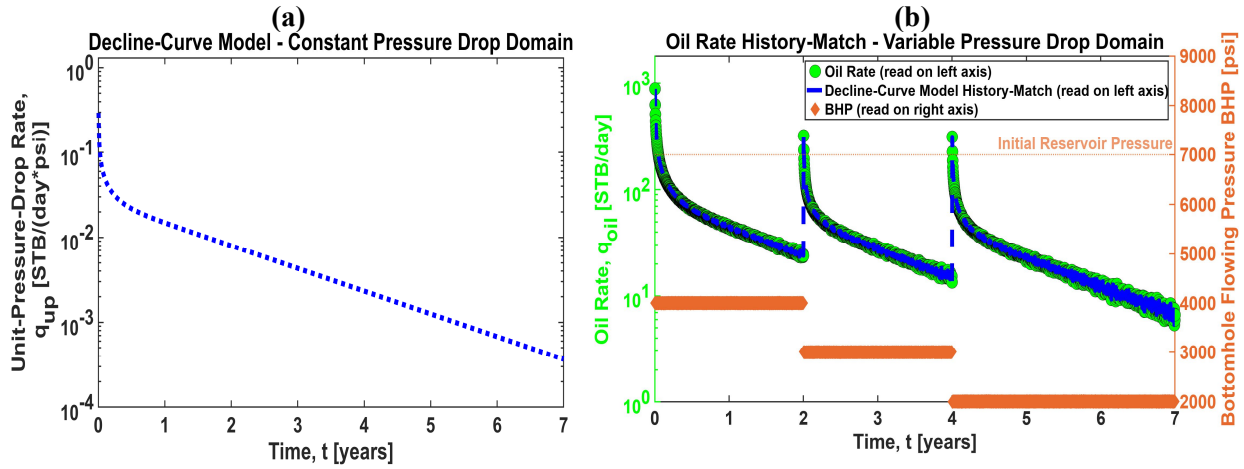

Fig. 1—Schematic illustrating the main idea of the variable pressure DCA method. The goal is to map a decline-curve model from (a) a constant-pressure domain to (b) variable pressure conditions to history-match and forecast the production of tight-oil wells.

To convert the decline-curve rate from constant- to variable-pressure domains, we apply the time-superposition principle.

$$\hat{q}(t;x,P_i,P_{wf}) = (P_i - P_{wf_1})\, q_{up}(t;x) + \sum_{k=2}^{n} \left[P_{wf_{k-1}} - P_{wf_k}\right] q_{up}(t - t_{k-1};x). \quad (1)$$

Equation 1 allows us to incorporate variable pressure drop conditions into our decline-curve model q_{up}. (defined in terms of rate per unit pressure). **Figure 2** illustrates the application of Eq. 1 for the case of an example tight-oil well. Figure 2 shows two rate histories: one corresponding to the actual well's history (green dots) and another showing the application of Eq. 1 using a decline-curve model (dashed blue curve). We use least-squares regression between the actual oil rate and $\hat{q}$ to obtain the decline-curve model's production history-match. This approach has been proposed by Ilk and Blasingame (2013) to account for variable pressure, but it typically yields poor history matches for the following reasons. First, Eq. 1 is very sensitive to errors in the data (data issues). Second, incorrect estimates in both the initial reservoir pressure P_i and the BHP produce errors in the rate response. These errors propagate forward in time leading to large oscillations in the variable-pressure rate response as shown by the dashed blue curve in Fig. 2.

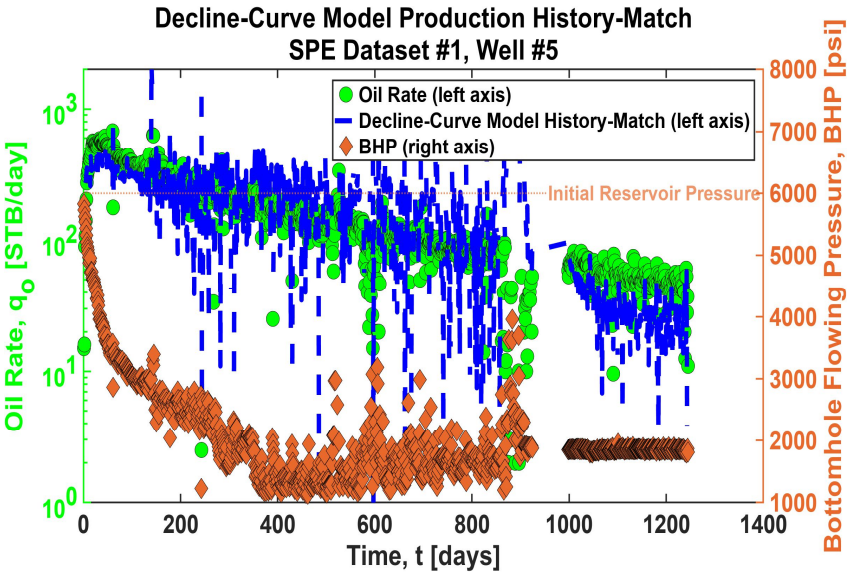

Fig. 2—Oil rate production history of a tight oil well (green dots) and production history-match using Eq. 1 with a decline-curve model (dashed blue lines). The model's history-match is very poor. Incorrect estimates in both the initial reservoir pressure P_i and the BHP produce errors in the rate response in Eq. 1. These errors propagate forward in time leading to large oscillations in the calculated rate.

To avoid these problems, we propose using the technique offered in this paper. This technique provides a fast and simple solution to incorporate variable BHP into any decline-curve model while addressing the following problems (data issues):

1. Incorrect estimate of initial reservoir pressure P_i.
2. Incorrect values of bottomhole flowing pressures P_{wf}.
3. Rate and bottomhole flowing pressure inconsistencies (e.g. flowing pressure increases and rate increases).

There are three main goals of the present method:

1. History-match the oil production using a decline-curve model while accounting for variable BHP.
2. Estimate the BHP history consistent with the decline-curve model history-match.
3. Estimate the initial reservoir pressure consistent with the decline-curve model history-match.

Workflow

This section details the workflow used in this study. There are three main steps: (1) production history-match, (2) pressure drop correction, and (3) initial reservoir pressure correction.

Step 1: Initialization

The first step selects a decline-curve model q_{up} for the analysis of the oil production. The decline-curve model should be defined in terms of rate per unit pressure drop (dimensions of rate divided by pressure). In addition, the method needs preliminary estimates $(l = 0)$ of the initial reservoir pressure $P_i^{(0)}$ and the bottomhole flowing pressure $P_{wf}^{(0)}$.

The algorithm requires a reasonable estimate for the BHP history. Ideally, flowing pressures should be measured using downhole pressure gauges but can be estimated using other means.

Step 2: N_p History Matching

The second step history matches the oil production using the time superposition equation with the cumulative production of the decline-curve model $N_{p_{up}}$. The cumulative production is a monotonic function that increases with time. Therefore, it is smoother than the rate history and provides a better history-match while dampening the effects of potential errors in the pressure drop estimates.

$$\widehat{N}_p(t;x,P_i,P_{wf}) = (P_i - P_{wf_1})N_{p_{up}}(t;x) + \sum_{k=2}^{n}[P_{wf_{k-1}} - P_{wf_k}]N_{p_{up}}(t - t_{k-1};x). \tag{2}$$

The least-squares regression of the cumulative production is given by Eq. 3.

$$x^{(l+1)} = \arg_x \min\left\{\left\|N_p(t) - \widehat{N}_p\left(t;x,P_i^{(l)},{P_{wf}}^{(0)}\right)\right\|_2^2\right\}. \tag{3}$$

The goal of this step is to estimate the decline-curve model parameters $\boldsymbol{x^{(l+1)}}$ and to use them in next step to correct/estimate the pressure drop.

Step 3: Pressure Drop Correction

This step applies rate-pressure deconvolution (Kuchuk et al. 2010) to estimate the pressure drop $\Delta P_{wf} = P_i - P_{wf}$ using the decline-curve model q_{up} and its parameters $x^{(l+1)}$ from step 2.

Equation 4 is an integrated form of the convolution integral (Ilk et al. 2007).

$$\int_0^t \Delta P_{wf}(t')q_{up}(t - t';x^{(l+1)})\,dt' = N_p(t)\,. \tag{4}$$

Considering a constant pressure drop for each time interval, Eq. 4 is discretized as follows.

$$\left.\begin{aligned}
&\Delta P_{wf_1}\int_0^{t_1} q_{up}(t_1 - t';x^{(l+1)})\,dt' + 0 + \cdots + 0 &&= N_p(t_1)\\
&\Delta P_{wf_1}\int_0^{t_1} q_{up}(t_2 - t';x^{(l+1)})\,dt' + \Delta P_{wf_2}\int_{t_1}^{t_2} q_{up}(t_2 - t';x^{(l+1)})\,dt' + \cdots + 0 &&= N_p(t_2)\\
&\qquad\qquad\vdots &&\\
&\sum_{k=1}^{n}\Delta P_{wf_k}\int_{t_{k-1}}^{t_k} q_{up}(t_n - t';x^{(l+1)})\,dt' &&= N_p(t_n)
\end{aligned}\right\} B^{(l+1)}\,\Delta P_{wf} = N_p, \tag{5}$$

where N_p and ΔP_{wf} are the cumulative production and the pressure drop vectors, respectively. The matrix $B^{(l+1)}$ contains the time integrals of the decline-curve model $q_{up}(t_k - t';x^{(l+1)})$.

The goal of this step is to get an estimate of the pressure drop ${\Delta P_{wf}}^{(l+1)}$. This estimate is then used in step 4 to correct/estimate the initial reservoir pressure.

$${\Delta P_{wf}}^{(l+1)} = \arg_{\Delta P_{wf}} \min\left\{\left\|N_p - B^{(l+1)}\Delta P_{wf}\right\|_2^2\right\}. \tag{6}$$

Step 4: Initial Reservoir Pressure Correction

This step estimates the initial reservoir pressure using the following least-squares optimization.

$$P_i^{(l+1)} = \arg_{P_i} \min \left\{ \left\| -\Delta P_{wf}{}^{(l+1)} + P_i - P_{wf}{}^{(0)} \right\|_2^2 \right\}. \quad (7)$$

Once Eq. 7 is solved, we return to step 2 with the estimated initial reservoir pressure, and we repeat steps 2 to 4 until:

$$\left\| \frac{P_i^{(l+1)} - P_i^{(l)}}{P_i^{(l)}} \right\|_2 \leq \text{Tolerance}. \quad (8)$$

The final outputs of the algorithm are: (a) the model's parameters $x^{(l+1)}$, (b) the initial reservoir pressure $P_i^{(l+1)}$, and (c) the pressure drop $\Delta P_{wf}{}^{(l+1)}$.

Step 5: Compute Rate History

The final step computes the oil rate history using Eq. 1 with the estimated model's parameters, the corrected initial reservoir pressure, and the corrected pressure drop. We convert the pressure drop into bottomhole flowing pressures using the pressure drop definition: $P_{wf}{}^{(l+1)} = -\Delta P_{wf}{}^{(l+1)} + P_i^{(l+1)}$.

$$\hat{q}\left(t; x^{(l+1)}, P_i^{(l+1)}, P_{wf}^{(l+1)}\right) = \left(P_i^{(l+1)} - P_{wf\,1}^{(l+1)}\right) q_{up}\left(t; x^{(l+1)}\right) + \sum_{k=2}^{n} \left[P_{wf\,k-1}^{(l+1)} - P_{wf\,k}^{(l+1)}\right] q_{up}\left(t - t_{k-1}; x^{(l+1)}\right). \quad (9)$$

Figure 3 is a flowchart illustrating the steps of the variable pressure drop DCA method.

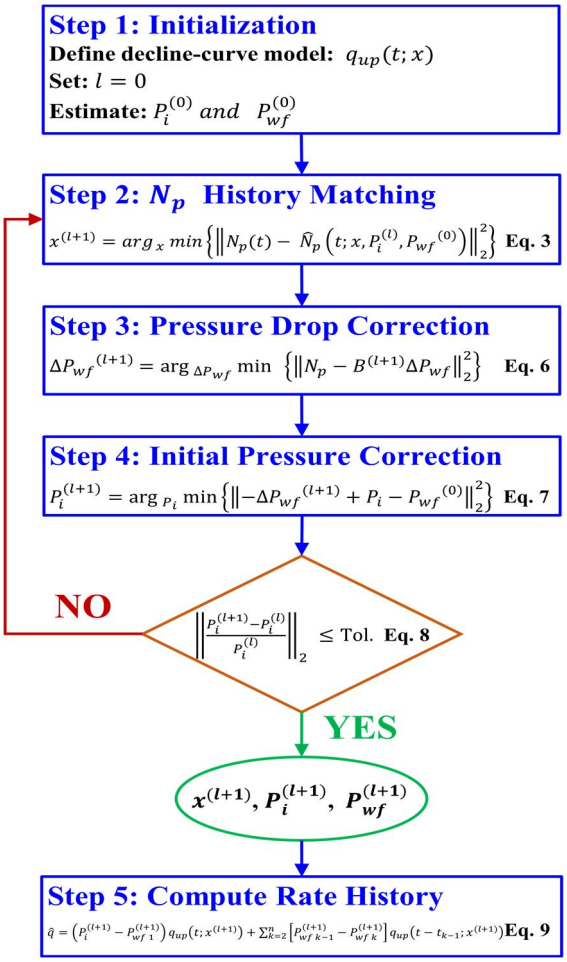

Fig. 3—Flowchart illustrating the steps of the variable pressure drop method. The workflow consists of three main steps: (I) production history-match (step 2), (II) pressure drop correction (step 3), and (III) initial reservoir pressure correction (step 4).

Computational Performance

The design of the algorithm meets three requirements: high stability, robustness, and speed. The above workflow achieves those requirements. The application of an efficient optimization technique helps us to achieve fast convergence. Currently, a typical analysis for an average well requires about **10 seconds** on a typical laptop computer. We expect much shorter execution times on more sophisticated hardware. Further improvements will shorten the computational time.

Validation With Synthetic Case

This study uses the 1-D constant-pressure solution of the diffusivity equation for a single-phase slightly compressible fluid along with time superposition (Eq. 1) to generate a synthetic example subject to variable BHP conditions.

The 1-D constant-pressure solution of the diffusivity equation for a single-phase slightly compressible fluid represents an idealized hydro-fractured well (**Fig. 4a**). It consists of n_f evenly-spaced, transverse planar hydraulic fractures that stimulate a rock volume around them. These stimulated rock volumes are equal for all hydro-fractures and constitute the stimulated rock volume (SRV) of the reservoir. The fractures and the well itself have infinite conductivity and thus, fluid that reaches them is instantly produced. In addition, we invoke the following model assumptions: (a) planar fractures of constant length $2x_f$ and height h_f and two producing faces, (b) flow is one-dimensional and perpendicular to the faces of the hydraulic fractures, (c) oil is a single component of constant properties at undersaturated conditions, (d) Darcy's law applies, (e) gravity and capillary forces are negligible, (e) constant irreducible water saturation S_{wi}, (f) an isothermal reservoir, (g) constant initial reservoir pressure P_i, (h) constant bottomhole flowing pressure P_{wf} at the fracture face, and (i) no-flow boundary at half the distance L between fractures.

The repetitive symmetry of Fig.4a allows solving the oil flow equation for a single half-fracture face (**Fig. 4b**). After obtaining the solution, we consider the oil flow from the remaining fractures by addition.

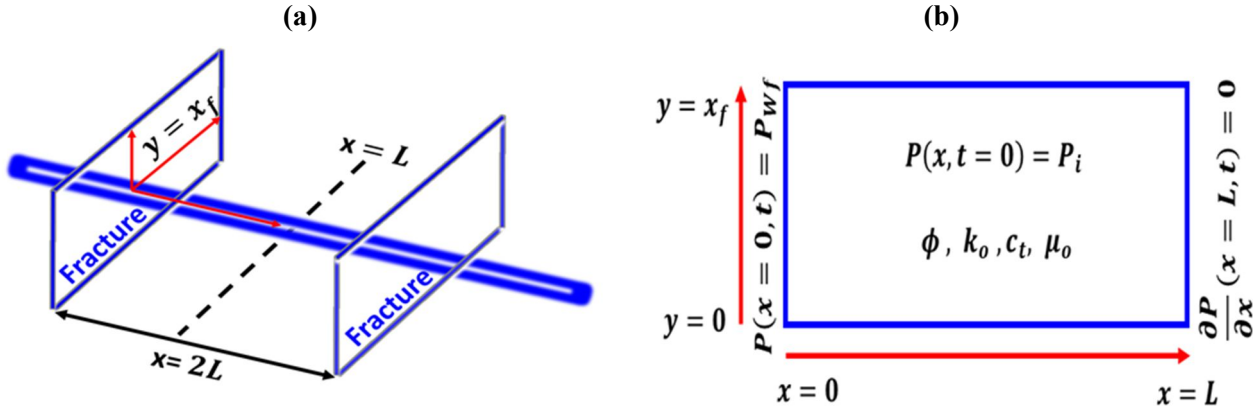

Fig. 4—(a) Idealized representation of a hydraulically-fractured well. (b) Top view of the simplified medium under study showing initial and boundary conditions.

Equation 10 is the dimensionless form of the pressure diffusivity equation (Walsh and Lake 2003) along with its initial (IC) and boundary (BC) conditions.

$$\frac{\partial P_D}{\partial t_D} = \frac{\partial^2 P_D}{\partial x_D^2}, \tag{10}$$

$$\text{IC: } P_D(t_D = 0, x_D) = 1, \qquad \text{BC1: } P_D(t_D, x_D = 0) = 0\,, \qquad \text{BC2: } \left(\frac{\partial P_D}{\partial x_D}\right)_{x_D=1} = 0.$$

The dimensionless variables in Eq. 10 are defined using the Shook et al. (1992) method.

Dimensionless pressure P_D

$$P_D = \frac{P - P_{wf}}{P_i - P_{wf}}. \tag{11}$$

Dimensionless coordinate x_D

$$x_D = \frac{x}{L}. \tag{12}$$

Dimensionless time t_D

$$t_D = \frac{t}{\tau}. \tag{13}$$

We solve Eq. 10 using the method of separation of variables (Hahn and Özişik 2012).

$$P_D(x_D, t_D) = \sum_{j=0}^{\infty} \left[\frac{4}{(2j+1)\pi}\right] \sin\left((2j+1)\frac{\pi}{2}\, x_D\right) e^{-\left[(2j+1)\frac{\pi}{2}\right]^2 t_D}. \tag{14}$$

The dimensionless rate q_D relates to the dimensionless pressure P_D as follows.

$$\begin{aligned} q_D(t_D) &= \left(\frac{\partial P_D}{\partial x_D}\right)_{x_D=0} \\ &= 2\sum_{j=0}^{\infty} e^{-\left[(2j+1)\frac{\pi}{2}\right]^2 t_D}. \end{aligned} \tag{15}$$

Equation 16 relates the unit-pressure-drop rate q_{up} to the dimensionless rate q_D. Eq. 16 is a decline-curve model with two parameters: a hydrocarbon pore volume V_p, and a characteristic time τ. These two parameters answer two important questions: how much oil is present V_p and how fast we can produce it τ (closely related to the time of end of transient flow).

$$q_{up}\left(t; V_p, \tau\right) = \frac{c_t V_p}{\tau} q_D(t/\tau). \tag{16}$$

The hydrocarbon pore volume and the characteristic time are defined by Eqs. 17 and 18, respectively.

$$V_p = 4\phi n_f h_f x_f L \tag{17}$$

$$\tau = \frac{L^2}{\alpha}, \qquad \alpha = \frac{k_o}{\phi \mu_o c_t}. \tag{18}$$

Table 1 defines the input reservoir and completion properties for the synthetic case under study.

Parameter	ϕ	k_o [nD]	μ_o [cP]	c_t [1/psi]	L [ft]	n_f	x_f [ft]	h_f [ft]	P_i [psi]
Value	0.078	218.10	0.30	2x10^{-5}	20	150	100	60	7,000

Table 1—Input reservoir and completion properties for the synthetic case.

Using the properties of Table 1 in Eq. 17 and Eq. 18 lead to the following values of the decline-curve model (Eq. 16) parameters V_p and τ:

- $V_p = 1$ MMSTB
- $\tau = 4$ years

Figure 5 shows the synthetic rate history (green dots) generated using Eqs. 1, 15, and 16 for the case of the bottomhole pressure history in the figure; the BHP history contains four distinct step changes (cyan lines). To test the robustness of our workflow, we superimpose noise on the pressure data in Fig. 5. This noise reflects possible uncertainty in the pressure measurements. Specifically, we consider an incorrect initial reservoir pressure of 8,000 psi (dashed red line) and the noisy BHP data shown by brown diamonds in Fig. 5. The error in the initial reservoir pressure is 15% and the error BHP ranges between 0-45%. For the synthetic case, Eq. 16 represents the decline-curve model.

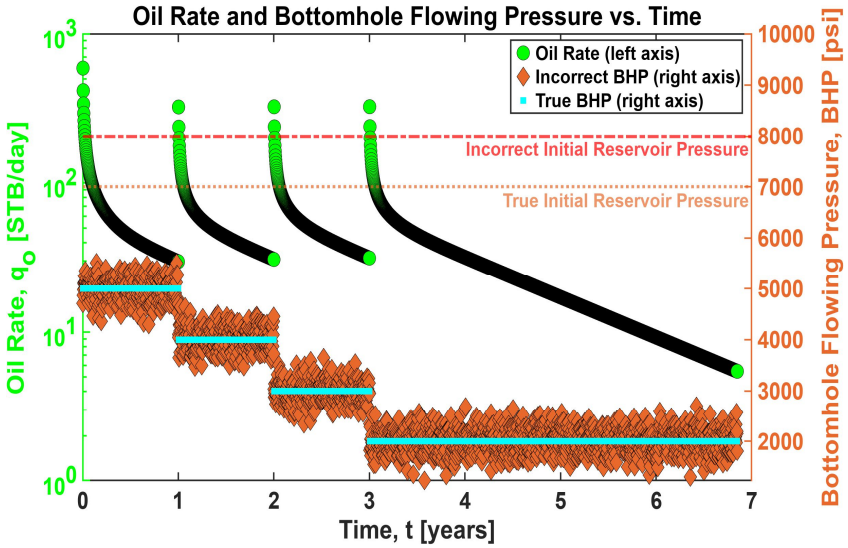

Fig. 5—Synthetic case oil rate history (green dots) generated using Eqs. 1, 15, and 16 with an initial reservoir pressure of 7,000 psi and a BHP history with step (cyan lines). We input incorrect initial reservoir pressure and BHP (dashed red line and the brown diamonds, respectively) to test the method's ability to accurately history-match the oil production and to estimate both the true initial reservoir pressure and the BHP. The error in the initial pressure is 15% and the error in the BHP ranges between 0-45%.

Figure 6 illustrates the results of the application of the method for the synthetic case of Fig. 5. The dashed blue curve is the oil rate history-match; the agreement with the oil production history is excellent. The dashed magenta line is the corrected initial reservoir pressure. This estimate coincides very closely with the true initial reservoir pressure. Finally, the dotted blue curve is the BHP history from the technique, which agrees well with the true BHP history.

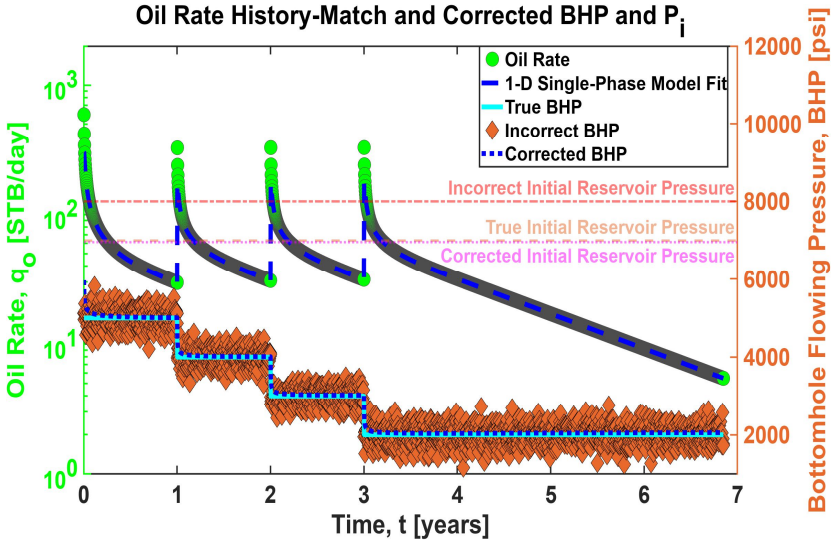

Fig. 6—Results of the application of the method for the synthetic case of Fig. 5. The dashed blue lines are the oil-rate history-match; the agreement with the oil production history is excellent. The dashed magenta line represents the corrected initial reservoir pressure estimated from the algorithm. This estimate coincides with the true initial reservoir pressure. Finally, the dotted blue curve is the BHP history estimated from the technique, which is in good agreement with the true BHP history.

Table 2 compares true and estimated initial reservoir pressure and model's parameters V_p and τ for the synthetic case. The relative errors for these quantities are less than 2%.

Parameter	True	Estimated	Relative Error [%]
P_i [psi]	7,000	6,950	-0.71
V_p [MMSTB]	4.00	4.07	1.75
τ [year]	1.00	0.99	-1.00

Table 2—Comparison between true and estimated initial reservoir pressure and model's parameters V_p and τ for the synthetic case. The relative errors for these quantities are less than 2%.

Tight-Oil Examples

This section illustrates the application of the variable pressure drop technique for tight-oil wells producing under variable pressure drop conditions. For each tight-oil well, we apply the method using three decline curve models: 1-D single-phase solution of the diffusivity equation for a slightly compressible fluid $q_{up\ SP}$ (Eq. 19), logistic growth model $q_{up\ LGM}$ (Eq. 20), and Arps hyperbolic relation $q_{up\ Hyp}$ (Eq. 21).

$$q_{up\ SP}\left(t; V_p, \tau\right) = \frac{c_t V_p}{\tau}\, 2 \sum_{j=0}^{\infty} e^{-\left[(2j+1)\frac{\pi}{2}\right]^2 \frac{t}{\tau}}. \tag{19}$$

$$q_{up\ LGM}\left(t; K_{up}, a_{LGM}, n_{LGM}\right) = \frac{K_{up} a_{LGM}\, n_{LGM}\, t^{n_{LGM}-1}}{(a_{LGM} + t^{n_{LGM}})^2}. \tag{20}$$

$$q_{up\ Hyp}\left(t; q_{i_{up}}, D_i, b\right) = \frac{q_{i_{up}}}{(1 + D_i b t)^{1/b}}. \tag{21}$$

These models are defined per unit pressure drop (rate divided by pressure). For this reason, the logistic growth model carrying capacity parameter K_{up} has dimensions of volume divided by pressure and the Arps hyperbolic initial rate parameter $q_{i_{up}}$ has dimensions of rate divided by pressure. In addition, this work constrains the Arps *b* parameter between 0 and 2.

Finally, we compare the history-matches, model's parameters, and production forecasts for each model with and without accounting for variable pressure drop conditions for each tight-oil well.

Well # 1

Figure 7 shows DCA results for the case of the 1-D single-phase model. Figure 7a compares rate history matches for the cases of including and ignoring variable pressure (dashed blue vs dotted red curves, respectively). The case of ignoring variable pressure is corresponds to conventional DCA where only rate-time data is considered. Accordingly, we sometimes refer to this method as the rate-time method, versus the pressure-rate-time method for the variable-pressure case. The variable-pressure case yields a much better history match; it effectively exhibits both the early-time ramp-up and the overall rate scatter. Figure 7b compares the forecasts for the cases of including and ignoring variable pressure. The forecasts are extended to 1400 days (3.8 years). The two cases exhibit markedly different predictions, with the variable-pressure case yielding a more conservative forecast.

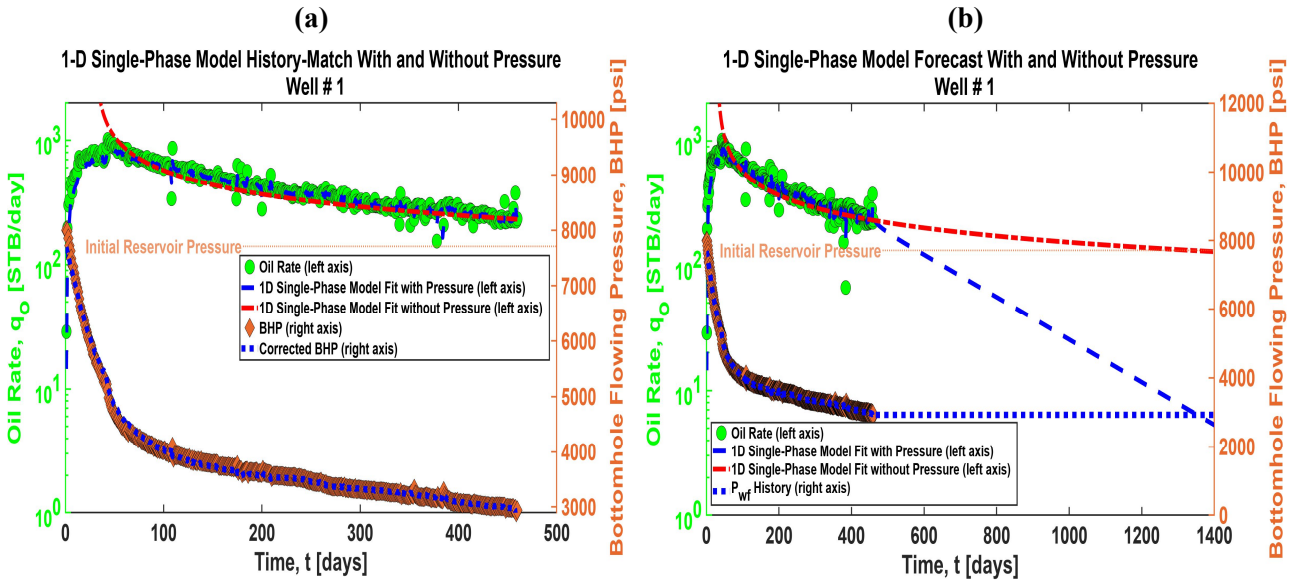

Fig. 7—Comparison of the production history-matches (Fig. 7a) and forecasts (Fig. 7b) using the 1-D single-phase model (Eq. 19) including variable BHP (dashed blue curve) and using only rate-time data (dotted-dashed red curve). The variable pressure method mimics both the early-time ramp-up and the scatter present in the oil rate in Fig. 7a. Figure 7b shows that incorporating variable pressure effects into the decline-curve model yields a production forecast that is less than the one using only rate-time data.

Table 3 compares the 1-D single-phase model parameters, 20-year EUR, and 20-year recovery factor (RF) values including variable pressure drop effects and using only rate-time data of Fig. 7. Including variable pressure effects lead to smaller model's parameters, 20-year EUR, and a realistic 20-year RF.

The marked differences between the two cases is related to the nature of the 1-D single-phase model. The model accounts for both transient and boundary-dominated flow (BDF) regimes. When the effects of variable pressure are considered, the model predicts the onset of BDF before 450 days; in contrast, when the effects of variable pressure are ignored, the model predicts BDF has not occurred, and therefore predicts a much greater τ and EUR.

Parameter	Pressure-Rate-Time	Rate-Time	Relative Difference [%]
V_p [MMSTB]	9.57	99.98	944.70
τ [year]	1.72	344.51	19,930
20-year EUR [MSTB]	247.86	817.08	229.70
20-year RF [%]	2.58	0.82	-68.40

Table 3—1-D single-phase model parameters, 20-year EUR, and 20-year recovery factor (RF) values including variable pressure drop effects (with pressure) and using only rate-time data (without pressure) of Fig. 7. Including variable pressure effects lead to smaller model's parameters and 20-year EUR, and a more realistic 20-year RF.

Figure 8 is analogous to Fig. 7 but considers the logistic growth model (Eq. 20). The dashed magenta and dotted-dashed red curves correspond to the cases including and ignoring variable pressure, respectively. The variable pressure case matches both the early-time ramp-up and the scatter present in the oil rate in Fig. 8a. In this case, incorporating variable pressure effects into the decline-curve model yields a slightly more conservative production forecast than the case of ignoring pressure (Fig. 8b).

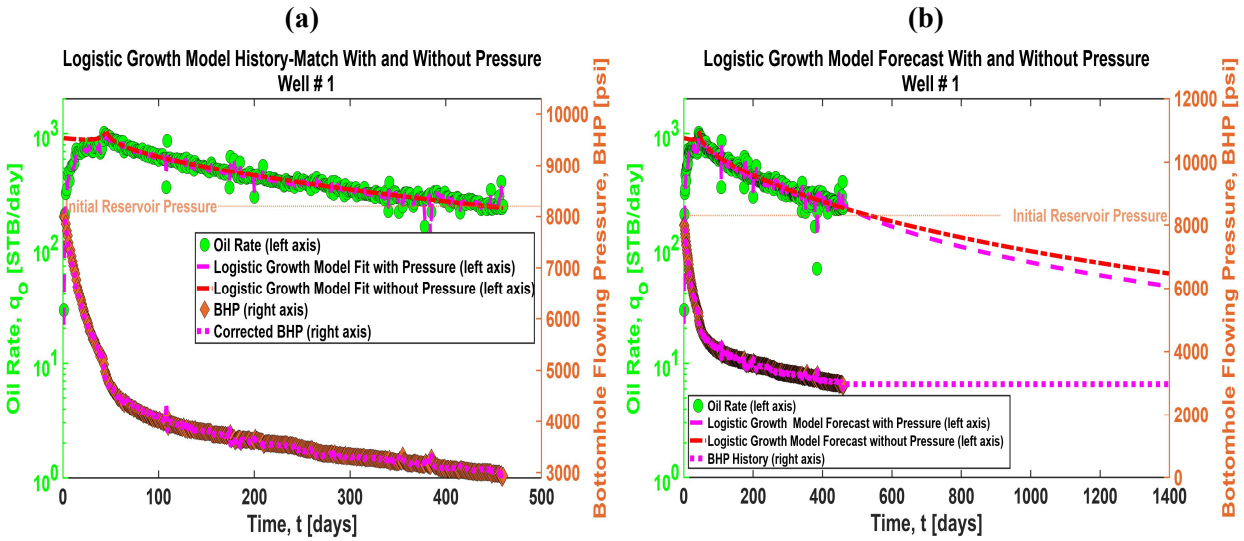

Fig. 8—Comparison of the production history-matches (Fig. 8a) and forecasts (Fig. 8b) using the logistic growth model (Eq. 20) including for variable BHP (dashed magenta curve) and using only rate-time data (dotted-dashed red curve). The variable pressure method mimics both the early-time ramp-up and the scatter present in the oil rate in Fig. 8a. In this case, the inclusion of variable pressure effects into the decline-curve model yields a slightly more conservative production forecast compared to using only rate-time data (Fig. 8b).

Table 4 compares the logistic growth model parameters and 20-year EUR values including variable pressure drop effects and using only rate-time data of Fig. 8. Including variable pressure effects leads to a slightly smaller 20-year EUR.

A comparison of Tables 3 and 4 reveals that the logistic growth model yields a greater EUR than the 1-D single-phase model for the case of including variable pressure (368 vs. 247 MSTB). The reason for this difference is explained by inherent differences in the models. The logistic growth model does not allow for a complete transition to BDF, unlike the 1-D single-phase model. This difference illustrates the importance of exercising careful consideration when selecting a decline-curve model.

Parameter	Pressure-Rate-Time	Rate-Time	Relative Difference [%]
K_{up} [STB/psi]	79.34	N/A	N/A
K [MSTB]	N/A	411.75	N/A
a_{LGM} [days^n]	87.44	358.85	310.40
n_{LGM} [dimensionless]	0.75	0.92	22.70
20-year EUR [MSTB]	368.56	375.16	1.80

Table 4—LGM parameters and 20-year EUR values including variable pressure drop effects (with pressure) and using only rate-time data (without pressure) of Fig. 8. Including variable pressure effects leads to a slightly smaller 20-year EUR.

Figure 9 is analogous to Figs. 7 and 8, but considers the Arps hyperbolic relation (Eq. 21). The black dashed and dotted-dashed red curves correspond to the cases of including and ignoring variable pressure, respectively. The variable pressure case exhibits both the early-time ramp-up and the scatter present in the oil rate in Fig. 9a. In this case, incorporating variable pressure effects into the decline-curve model yields a more conservative production forecast than the case of considering only rate-time data (Fig. 9b).

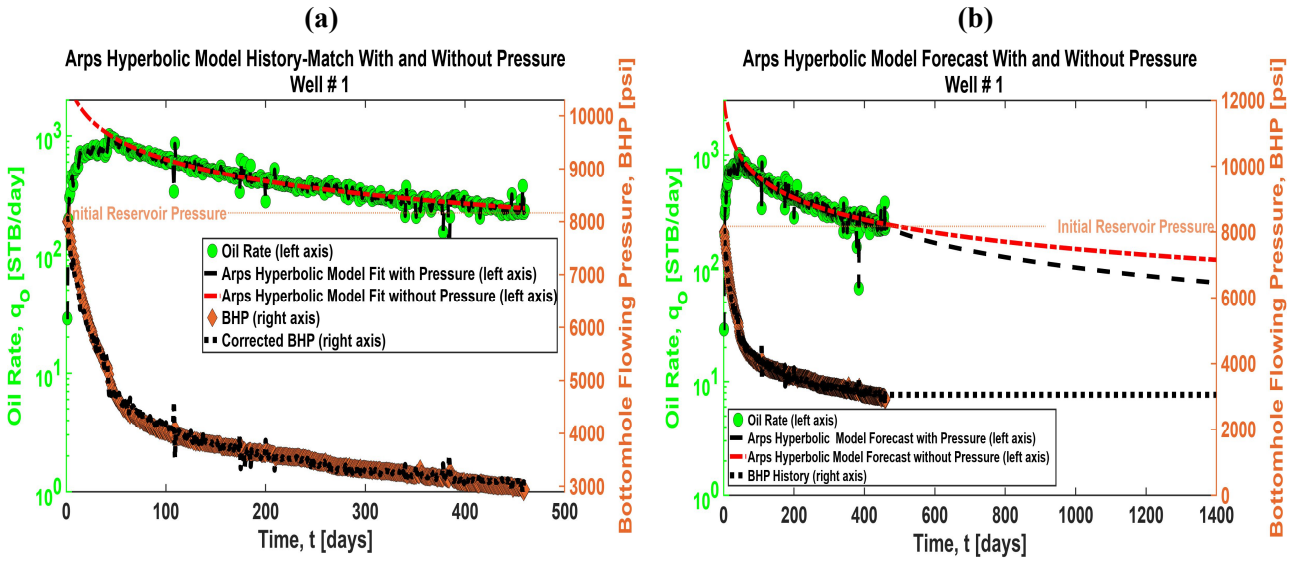

Fig. 9—Comparison of the production history-matches (Fig. 9a) and forecasts (Fig. 9b) using the Arps hyperbolic model (Eq. 21) including variable BHP (dashed black curve) and using only rate-time data (dotted-dashed red curve). The variable pressure method mimics both the early-time ramp-up and the scatter present in the oil rate in Fig. 9a. Incorporating variable pressure effects into the decline-curve model yields a production forecast that is less than the one using only rate-time data (Fig. 9b).

Table 5 compares the Arps hyperbolic model parameters and 20-year EUR values including variable pressure drop effects and using only rate-time data of Fig. 9. Including variable pressure effects yield a smaller b value and a smaller 20-year EUR.

The EUR differences between Table 3, 4, and 5 is readily explained by the differences in the models. The EUR of the Arps model (504 MSTB) is much greater than those of the 1-D single-phase model (247 MSTB) or logistic growth model (368 MSTB) because the Arps model is inherently limited to one flow regime, thereby precluding full BDF. The difference between the models again underscores the importance of careful consideration when selecting a model.

Parameter	Pressure-Rate-Time	Rate-Time	Relative Difference [%]
$q_{i_{up}}$ [STB/(day psi)]	0.50	N/A	N/A
q_i [MSTB/day]	N/A	199.90	N/A
D_i [1/days]	0.04	0.01	-75.00
b [dimensionless]	1.16	1.53	31.90
20-year EUR [MSTB]	504.77	699.62	38.60

Table 5—Arps hyperbolic model parameters and 20-year EUR values including variable pressure drop effects and using only rate-time data of Fig. 9. Including variable pressure effects yield a smaller b value and a smaller 20-year EUR.

Well # 2

One important difference between this well and Well #1 is that this well exhibits substantial BHP variation over a longer time period than Well #1 (250 days versus 50 days).

Figure 10 considers the 1-D single-phase model. The dashed blue and dotted-dashed red curves correspond to the cases including and ignoring variable pressure, respectively. The variable pressure case matches the trends and scatter in the rate data much better than the rate-time case. Figure 10b shows that incorporating variable pressure effects yields a more conservative production forecast than the rate-time case.

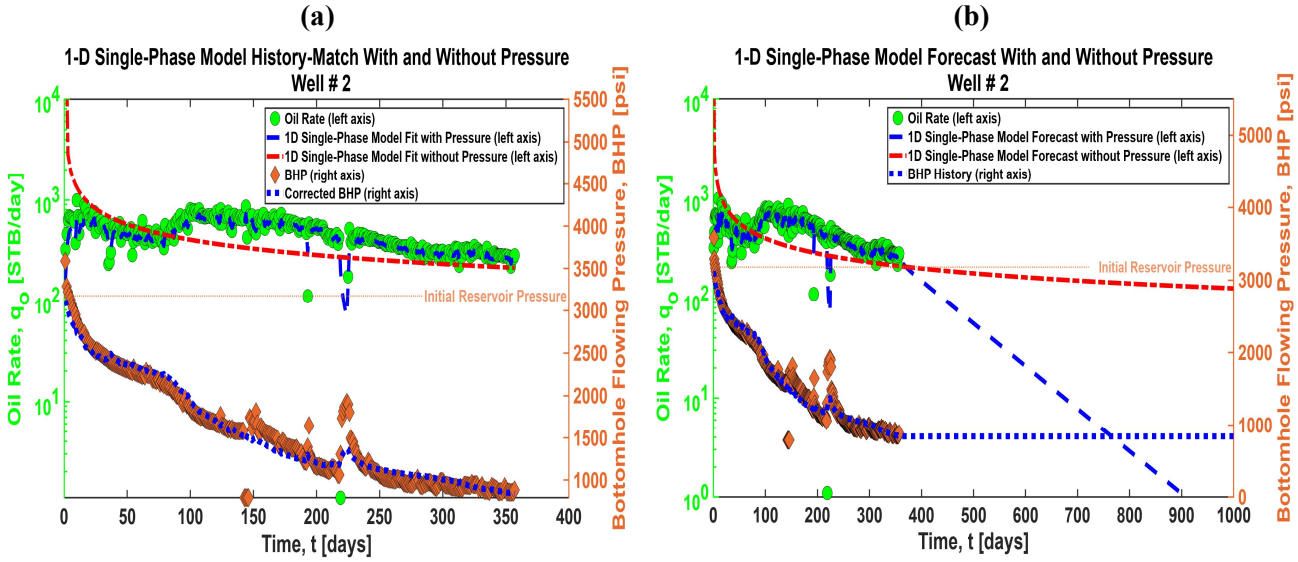

Fig. 10—Production history-matches (a) and forecasts (b) using the 1-D single-phase model (Eq. 19) including variable BHP (dashed blue curve) and using only rate-time data (dotted-dashed red curve). The variable pressure case matches the rate history much better than the rate-time case-(Fig. 10a). Figure 10b shows that the former case yields a more conservative forecast than the latter case.

Table 6 compares the 1-D single-phase model parameters, 20-year EUR, and 20-year RF values including variable pressure drop effects and using only rate-time data of Fig. 10. Including variable pressure effects yield smaller model's parameters, 20-year EUR, and a realistic 20-year RF.

Parameter	Pressure-Rate-Time	Rate-Time	Relative Difference [%]
V_p [MMSTB]	6.76	100	1,379.00
τ [year]	0.69	544.7	78,842.00
20-year EUR [MSTB]	181.18	682.38	276.60
20-year RF [%]	2.68	0.68	-74.50

Table 6—1-D single-phase model parameters, 20-year EUR, and 20-year recovery factor (RF) values including variable pressure effects and using only rate-time data of Fig. 10. Including variable pressure effects yield smaller model's parameters, 20-year EUR, and a realistic 20-year RF.

Figure 11 shows results for the logistic growth model (Eq. 20). The dashed magenta and dotted-dashed red curves show the results for the cases including and ignoring variable pressure, respectively. Again, the variable-pressure case matches the bumps and scatter in the rate history much better than the case ignoring variable pressure. Incorporating variable pressure effects into the decline-curve model yields a more conservative production forecast compared to using only rate-time data (Fig. 11b).

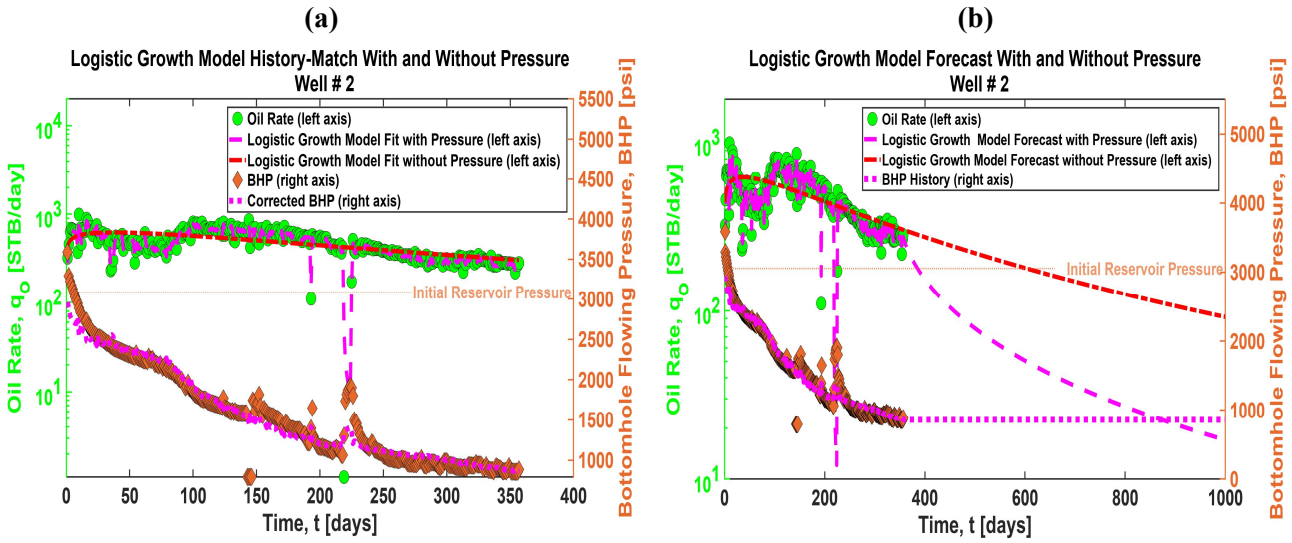

Fig. 11—Comparison of the production history-matches (a) and forecasts (b) using the logistic growth model (Eq. 20) including variable BHP (dashed magenta curve) and using only rate-time data (dotted-dashed red curve). The variable pressure method mimics the bumps and scatter present in the oil rate in Fig. 11a. In this case, the inclusion of variable pressure effects into the decline-curve model yields a smaller production forecast compared to the one using only rate-time data (Fig. 11b).

Table 7 compares the logistic growth model parameters and 20-year EUR values including variable pressure drop effects and using only rate-time data of Fig. 11. Including variable pressure effects yield a smaller 20-year EUR.

Parameter	Pressure-Rate-Time	Rate-Time	Relative Difference [%]
K_{up} [STB/psi]	100.83	N/A	N/A
K [MSTB]	N/A	392.22	N/A
a_{LGM} [days^n]	36.61	1,000	2,631.50
n_{LGM} [dimensionless]	0.89	1.13	27.00
20-year EUR [MSTB]	217.50	375.47	72.60

Table 7—Logistic model parameters and 20-year EUR values including variable pressure drop effects and using only rate-time data of Fig. 11. Including variable pressure effects yield a smaller 20-year EUR.

Figure 12 shows the results for the Arps hyperbolic model (Eq. 21). The dashed magenta and dotted-dashed red curves correspond to the cases including and ignoring variable pressure, respectively. The variable pressure case matches the bumps and scatter present in the oil rate in Fig. 12a. Incorporating variable pressure effects into the decline-curve model yields a more conservative production forecast than the case of ignoring pressure (Fig. 12b).

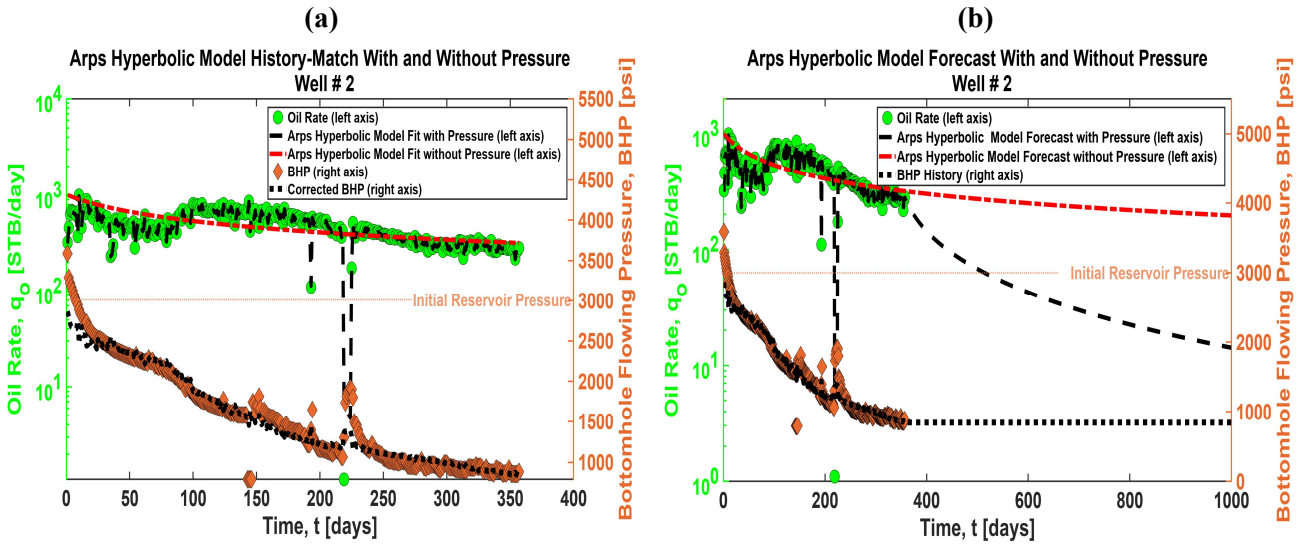

Fig. 12—Comparison of the production history-matches (Fig. 12a) and forecasts (Fig. 12b) using the Arps hyperbolic model (Eq. 21) including variable BHP (dashed black curve) and using only rate-time data (dotted-dashed red curve). The variable pressure method mimics the bumps and scatter present in the oil rate in Fig. 12a. Incorporating variable pressure effects into the decline-curve model yields a more conservative production forecast compared to using only rate-time data (Fig. 12b).

Table 8 compares the Arps hyperbolic model parameters and 20-year EUR values including variable pressure drop effects and using only rate-time data of Fig. 12. The variable pressure drop method yields a b value smaller than one, meaning that the well is in boundary-dominated flow, and a smaller 20-year EUR.

Parameter	Pressure-Rate-Time	Rate-Time	Relative Difference [%]
$q_{i_{up}}$ [STB/(day psi)]	2.41	N/A	N/A
q_i [MSTB/day]	N/A	1.00	N/A
D_i [1/days]	0.05	0.01	-80.00
b [dimensionless]	0.560	2.00	257.10
20-year EUR [MSTB]	211.32	1,003.60	374.90

Table 8—Arps hyperbolic model parameters and 20-year EUR values including variable pressure drop effects and using only rate-time data of Fig. 12. The variable pressure drop method yields a b value smaller than one, meaning that the well is in boundary-dominated flow, and a smaller 20-year EUR.

Well # 3

This well, like Well #2, exhibits a relatively long period of declining BHP. Figures 13, 14, and 15 in this section are analogous in format to figures for the previous wells.

Figure 13 shows the results for the 1-D single-phase model (Eq. 19). The dashed blue and dotted-dashed red curves correspond the cases including and ignoring variable pressure, respectively. The variable pressure case matches the bumps and scatter in the oil rate much better than the case ignoring variable pressure (Fig. 13a). Figure 13b shows that the case of including variable pressure yields a more conservative production forecast than the case ignoring variable pressure.

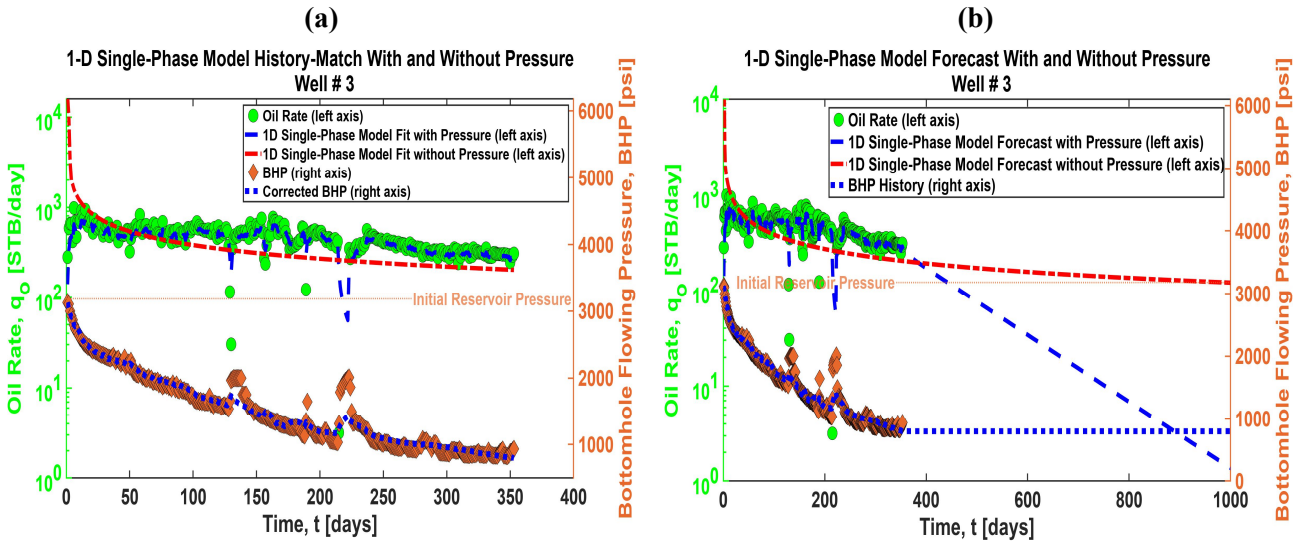

Fig. 13—Production history-matches (a) and forecasts (b) using the 1-D single-phase model (Eq. 19) including variable BHP (dashed blue curve) and using only rate-time data (dotted-dashed red curve). The variable pressure method has both the bumps and scatter present in the oil rate while the rate-time model fit cannot history-match the oil production (Fig. 13a). Figure 13b shows that incorporating variable pressure effects into the decline-curve model yields a conservative production forecast compared to using only rate-time data.

Table 9 compares the 1-D single-phase model parameters, 20-year EUR, and 20-year RF values including variable pressure drop effects and using only rate-time data of Fig. 13. Including the variable pressure effects leads to smaller model's parameters, 20-year EUR, and a realistic 20-year RF.

Parameter	Pressure-Rate-Time	Rate-Time	Relative Difference [%]
V_p [MMSTB]	6.67	99.72	1,395.10
τ [year]	0.84	864.95	102,870
20-year EUR [MSTB]	183.04	653.82	257.20
20-year RF [%]	2.74	0.66	-76.10

Table 9—1-D single-phase model parameters, 20-year EUR, and 20-year RF values including variable pressure drop effects and using only rate-time data of Fig. 13. Including the variable pressure effects leads to smaller model's parameters, 20-year EUR, and a realistic 20-year RF.

Figure 14 shows the results for the logistic growth model (Eq. 20). The dashed magenta and dotted-dashed red curves correspond to the cases including variable BHP and ignoring variable BHP, respectively. The variable pressure case matches both the bumps and scatter present in the oil rate history in Fig. 14a much better than the case ignoring variable pressure. Including variable BHP effects leads to a more conservative production forecast than the case of ignoring BHP (Fig. 14b).

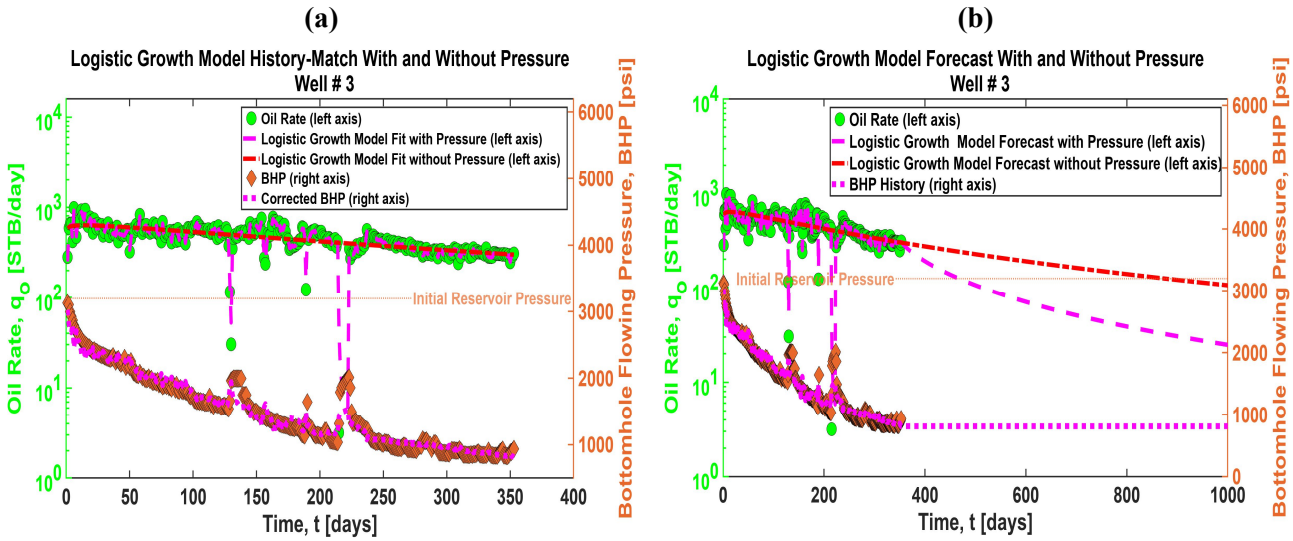

Fig. 14—Comparison of the production history-matches (a) and forecasts (b) using the logistic growth model (Eq. 20) including variable BHP (dashed magenta curve) and using only rate-time data (dotted-dashed red curve). The variable pressure method mimics both the bumps and scatter present in the oil rate in Fig. 14a. Including variable BHP effects leads to a conservative production forecast compared to using only rate-time data (Fig. 14b).

Table 10 compares the logistic growth model parameters and 20-year EUR values including variable pressure drop effects and using only rate-time data of Fig. 14. Including pressure effects yield a smaller 20-year EUR.

Parameter	Pressure-Rate-Time	Rate-Time	Relative Difference [%]
K_{up} [STB/psi]	98.73	N/A	N/A
K [MSTB]	N/A	437.84	N/A
a_{LGM} [days^n]	68.83	772.75	1,022.70
n_{LGM} [dimensionless]	0.92	1.04	13.00
20-year EUR [MSTB]	235.07	408.01	73.60

Table 10—Logistic model parameters and 20-year EUR values including variable pressure drop effects and using only rate-time data of Fig. 14. Including pressure effects yield a smaller 20-year EUR.

Figure 15 shows the results using the Arps hyperbolic relation (Eq. 21). The black dashed and dotted-dashed red curves correspond to the cases including and ignoring variable BHP, respectively. The variable pressure case matches both the bumps and scatter in the rate history in Fig. 15a much better than the case ignoring the pressure variations. Incorporating variable pressure effects into the decline-curve model yields a more conservative production forecast than the case ignoring variable pressure (Fig. 15b).

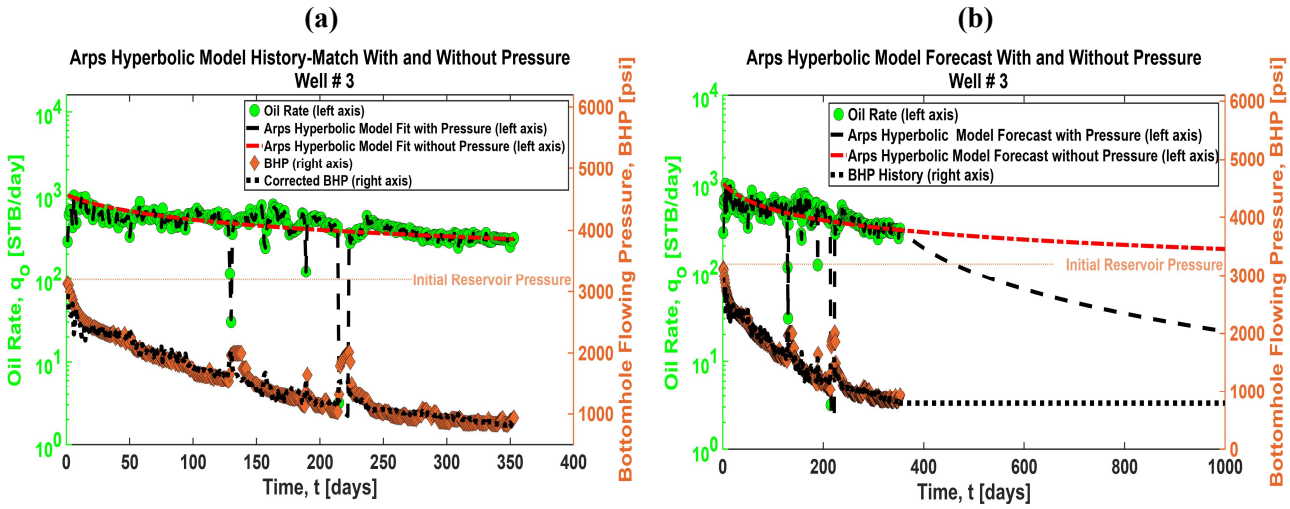

Fig. 15—Comparison of the production history-matches (Fig. 15a) and forecasts (Fig. 15b) using the Arps hyperbolic model (Eq. 21) including variable BHP (dashed black curve) and using only rate-time data (dotted-dashed red curve). The variable pressure method mimics the bumps and scatter present in the oil rate in Fig. 15a. Incorporating variable pressure effects into the decline-curve model yields a more conservative production forecast compared to using only rate-time data (Fig. 15b).

Table 11 compares the Arps hyperbolic model parameters and 20-year EUR values including variable pressure drop effects and using only rate-time data of Fig. 15. Incorporating variable pressure effects yield a b value smaller than one, meaning that the well is in boundary-dominated flow, and a smaller 20-year EUR.

Parameter	Pressure-Rate-Time	Rate-Time	Relative Difference [%]
$q_{i_{up}}$ [STB/(day psi)]	1.37	N/A	N/A
q_i [MSTB/day]	N/A	0.80	N/A
D_i [1/days]	0.03	0.01	-66.70
b [dimensionless]	0.55	2.00	263.60
20-year EUR [MSTB]	223.99	1,038.90	364.30

Table 11—Arps hyperbolic model parameters and 20-year EUR values including variable pressure drop effects and using only rate-time data of Fig. 15. The variable pressure drop method yields a b value smaller than one meaning that the well is in boundary-dominated flow, and a smaller 20-year EUR.

Implications to Traditional Rate-Transient Analysis (RTA)

The method presented in this paper uses pressure-rate-time data to match the rate history and to estimate the well's future production. The goal of popular RTA software programs is similar but they employ a different workflow, one that characteristically includes different diagnostic plots, such as a plot of normalized pressure versus square root of time, and requires the interpretation of an experienced reservoir engineer. If our method is applied using the 1-D single-phase decline-curve model, it mimics RTA but does not require an interpretation of diagnostic plots and does not suffer from some of the limitations of traditional RTA. Several investigators have recently discussed those limitations (Chaudhary and Lee 2016; Bowie and Ewert 2020; Carlsen et al. 2021). For instance, the present technique does not assume rate normalization since it solves the convolution integral to rigorously account for BHP changes. See Chaudhary and Lee (2016) for a discussion of the limitations of rate normalization. In summary, this method can be used as a supplement to RTA but without some of its limitations and intermediate graphing steps.

Conclusions

This paper presents a new method to incorporate variable bottomhole pressures into decline-curve analysis using any decline-curve model. The technique is remarkably stable, robust, and fast (about 10 seconds per well). It consistently matches the rate better than conventional DCA, which ignores changes in the BHP.

The conclusions of this work are the following.

- For the synthetic example, the variable pressure DCA method provides an excellent history-match to the oil production history despite the presence of errors in both the initial reservoir pressure and the BHP history (Fig. 6). In addition, the method estimates the true model parameters and initial reservoir pressure within 2% error (Table 2).
- The proposed method for correcting initial pressure and BHP measurements (Fig. 3) gives a way to infer possible corrections to errors present in the initial reservoir pressure and BHP history for tight-oil wells and to estimate the true or actual initial pressure and BHP (Fig. 6).
- For the tight-oil examples, we show that including variable pressure conditions into decline curve models lead to more accurate production history-matches and smaller 20-year EUR values compared to the analysis of decline-curve models using only rate time data, see Figs. 7-15 and Tables 3-11.
- The analysis of tight-oil well examples #2 and #3 using the 1-D single phase and the Arps hyperbolic relation (Figs. 9 and 15) stress the importance of incorporating variable pressure conditions for correct flow regime identification. Rate-time analysis might lead to incorrect τ and b values (for the 1-D single-phase and the Arps hyperbolic models, respectively) and thus, inaccurate flow regime characterization and misleading production forecasts because of BHP variations, see Tables 6, 8, and 9, 11, respectively.
- The present method uses pressure-rate-time data to match the rate history and has similar goals of traditional RTA. However, the method does not: (a) require interpretation of diagnostic plots and (b) suffer from some of the limitations of RTA. This method can be used as a supplement to traditional RTA but without some of its limitations and intermediate graphing steps.

Nomenclature

a_{LGM}	=	logistic growth model parameter, $t^{n_{LGM}}$, $day^{n_{LGM}}$
b	=	Arps model b parameter, dimensionless
B	=	convolution matrix for estimating pressure drops, t^2 L^4/m, STB/psi
c_t	=	total compressibility, Lt^2/m, psi^{-1}
D_i	=	Arps model initial decline rate parameter, t^{-1}, day^{-1}
h_f	=	fracture height, L, ft
j	=	iteration index, dimensionless
k	=	time iteration index, dimensionless
k_o	=	oil phase permeability, L^2, nD
K	=	logistic growth model carrying capacity parameter, L^3, MSTB
K_{up}	=	logistic growth model carrying capacity parameter per unit pressure, t^2 L^4/m, STB/psi
l	=	iteration index, number
L	=	half distance between adjacent fractures, L, ft
L_T	=	total lateral length, L, ft
N_p	=	oil cumulative production, L^3, MSTB
$\widehat{N}_p$	=	model estimate of the oil cumulative production, L^3, MSTB
n	=	number of time production data values, number
a_{LGM}	=	logistic growth model parameter, dimensionless

n_f = total number of fractures, number
P = reservoir pressure, m/Lt^2, psi
P_i = initial reservoir pressure, m/Lt^2, psi
P_{wf} = bottomhole flowing pressure, m/Lt^2, psi
$\hat{q}$ = model estimate of the oil rate, L^3/t, STB/day
q_i = Arps model initial rate parameter, L^3/t, STB/day
$q_{i_{up}}$ = Arps model initial rate parameter per unit pressure, L^{2}t/m, STB/(psi day)
q_D = dimensionless rate, dimensionless
q_o = gas rate at standard conditions, L^3/t, STB/day
q_{up} = unit-pressure-drop oil rate, t L^4/m, STB/(day*psi)
S_{wi} = irreducible water phase saturation, fraction
t = time, t, day
t_D = hydrocarbon pore volume parameter, L^3, MMSTB
t_D = dimensionless time, dimensionless
x = model's parameters
x_D = dimensionless space coordinate, dimensionless
x_f = fracture half-length, L, ft
α = diffusion coefficient, L^2/t, ft^2/day
ΔP_{wf} = pressure drop, m/Lt^2, psi
μ_o = oil phase viscosity, m/Lt, cP
π = 3.14159, number
τ = characteristic time parameter, t, year
ϕ = porosity, fraction
$\| \ \|_2$ = Euclidean norm

Superscripts and subscripts

D = dimensionless
f = fracture
Hyp = Arps hyperbolic decline-curve model
i = initial condition
j = index
k = index for production time values
LGM = logistic growth decline-curve model
l = iteration index
o = oil phase
SP = 1-D constant-pressure single-phase slightly compressible decline-curve model
up = unit-pressure-drop
wf = bottom-hole flowing pressure conditions
$\widehat{\ }$ = model estimate

Abbreviations

BC = boundary condition
BHP = bottomhole flowing pressure
DCA = decline-curve analysis
EUR = estimated ultimate recovery
IC = initial condition
M = thousand
MM = million
RF = recovery factor
RTA = rate-transient analysis

Acknowledgements

This work was partially funded by the State of Texas Advanced Resource Recovery Program (STARR) at the Bureau of Economic Geology. Larry W. Lake holds the Sharon and Shahid Ullah Chair at the Center for Subsurface Energy and the Environment at The University of Texas at Austin. Mark P. Walsh is a Research Fellow at the Hildebrand Department of Petroleum and Geosystems Engineering at The University of Texas at Austin and an oil and gas consultant in Austin, Texas. Publication was authorized by the director of the Bureau of Economic Geology.

References

Arps, J. J. 1945. Analysis of Decline Curves. *Transactions of the AIME* **160** (1): 228-247. SPE-945228-G.

Aster, R., Borchers, B., and Thurber, C. 2019. Parameter Estimation and Inverse Problems, third edition, Amsterdam, The Netherlands: Elsevier.

Bowie, B. and Ewert, J. 2020. Numerically Enhanced RTA Workflow - Improving Estimation of Both Linear Flow Parameter and Hydrocarbons in Place. Presented at the SPE/AAPG/SEG Unconventional Resources Technology Conference, Virtual, 20-22 July. URTEC-2020-2967-MS. https://doi.org/10.15530/urtec-2020-2967

Carlsen, M. L., Bowie, B., Dahouk, M. M., et al. 2021. Numerical RTA in Tight Unconventionals. Presented at the SPE Annual Technical Conference and Exhibition, Dubai, UAE, 21-24 September. SPE-205884-MS. https://doi.org/10.2118/205884-MS

Chaudhary, N. L. and Lee, J. W. 2016. An Enhanced Method to Correct Rate Data for Variations in Bottom-Hole Pressure. Presented at the SPE/IAEE Hydrocarbon Economics and Evaluation Symposium, Houston, Texas, USA, 17-18 May. SPE-179959-MS. https://doi.org/10.2118/179959-MS

Clark, A. J., Lake, L. W., and Patzek, T. W. 2011. Production Forecasting With Logistic Growth Models. Presented at the SPE Annual Technical Conference and Exhibition, Denver, Colorado, USA, 30 October-2 November. SPE-144790-MS. https://doi.org/10.2118/144790-MS

Collins, P., Ilk, D., and Blasingame, T. A. 2014. Practical Considerations for Forecasting Production Data in Unconventional Reservoirs — Variable Pressure Drop Case. Presented at the SPE Annual Technical Conference and Exhibition, Amsterdam, The Netherlands, 27-29 October. SPE-170945-MS. https://doi.org/10.2118/170945-MS

Hahn, D. W. and Özişik, M. N. 2012. *Heat Conduction*, third edition, NJ, USA, Wiley.

Hansen, C. 2002. Deconvolution and Regularization with Toeplitz Matrices. *Numerical Algorithms* **29**: 323–378. https://doi.org/10.1023/A:1015222829062

Ilk, D., Valko, P., and Blasingame, T. 2007. A Deconvolution Method Based on Cumulative Production for Continuously Measured Flowrate and Pressure Data. Presented at the Eastern Regional Meeting, Lexington, Kentucky USA, 17-19 October. SPE-111269-MS. https://doi.org/10.2118/111269-MS

Ilk, D., Rushing, J. A., Perego, A. D., et al. 2008. Exponential vs. Hyperbolic Decline in Tight Gas Sands: Understanding the Origin and Implications for Reserve Estimates Using Arps Decline Curves. Presented at the SPE Annual Technical Conference and Exhibition, Denver, Colorado, USA, 21-24 September. SPE-116731-MS. https://doi.org/10.2118/116731-MS

Ilk, D. and Blasingame, T. A. 2013. Decline Curve Analysis for Unconventional Reservoir Systems — Variable Pressure Drop Case. Presented SPE Unconventional Resources Conference Canada, Calgary, Alberta, Canada, 5-7 November. SPE-167253-MS. https://doi.org/10.2118/167253-MS

Kuchuk, F. J., Hollaender, F., Gok, I. M. et al. 2005. Decline Curves from Deconvolution of Pressure and Flow-Rate Measurements for Production Optimization and Prediction. Presented at the SPE Annual

Technical Conference and Exhibition, Dallas, Texas, October. SPE-96002-MS. https://doi.org/10.2118/96002-MS

Kuchuk, F. J., Hollaender, F., and Onur, M. 2010. *Pressure Transient Formation and Well Testing: Convolution, Deconvolution and Non-Linear Estimation*. Developments in Petroleum Science 57. First edition, Amsterdam, The Netherlands: Elsevier.

Male, F. R., Marder, M., Browning, J., et al. 2016. Production Decline Analysis in the Eagle Ford. Presented at the Unconventional Resources Technology Conference, San Antonio, Texas, USA, 1-3 August. URTEC-2458308-MS. https://doi.org/10.15530/URTEC-2016-2458308

MATLAB. 2020. version 9.9.0.1592791 (R2020b), Natick, Massachusetts: The MathWorks Inc.

Patzek, T. W., Male, F., and Marder, M. 2013. Gas Production in the Barnett Obeys a Simple Scaling Theory. *Proceedings of the Natural Academy of Sciences* **110** (49): 19731-19736. https://doi.org/10.1073/pnas.1313380110\

Shook, M., Li, D., and Lake, L. W. 1992. Scaling Immiscible Flow Through Permeable Media by Inspectional Analysis. *In Situ* **16** (4): 311-349.

Valko, P. P. 2009. Assigning Value to Stimulation in the Barnett Shale: A Simultaneous Analysis of 7000 Plus Production Histories and Well Completion Records. Society of Petroleum Engineers. Presented at SPE Hydraulic Fracturing Technology Conference, The Woodlands, Texas, USA, 19-21 January. SPE-119369-MS. https://doi.org/10.2118/119369-MS

Walsh, M. P. and Lake, L. W. 2003. *A Generalized Approach to Primary Hydrocarbon Recovery*, first edition. Amsterdam, The Netherlands: Elsevier.

Wattenbarger, R. A., El-Banbi, A. H., Villegas, M. E., et al. 1998. Production Analysis of Linear Flow Into Fractured Tight Gas Wells. Presented at the SPE Rocky Mountain Regional/Low-Permeability Reservoirs Symposium. Denver, Colorado, USA, 5-8 April. SPE-39931-MS. https://doi.org/10.2118/39931-MS